Electronic Supplementary Material (ESI) for Journal of Materials Chemistry A.
This journal is © The Royal Society of Chemistry 2020

Supplementary Information

In-situ Filling Hydrogel Electrolyte into Robust Carbon Sponge: A Type Omni-Healable Electrode for Flexible Supercapacitors

*Liaoyuan Xia, * [a] [1] Le Huang, [a] [1] Yan Qing, [a] Xueqin Zhang,[a] Yiqiang Wu,[a] Wenping Jiang, [a] and Xihong Lu,* [b,c]*

a. Hunan Province Key Laboratory of Materials Surface & Interface Science and Technology, Central South University of Forestry and Technology, Changsha 410004, P. R. China.
E-mail: xly1516@126.com

b. School of Applied Physics and Materials, Wuyi University, Jiangmen 529020, P. R. China.
E-mail: luxh6@mail.sysu.edu.cn

c. MOE of the Key Laboratory of Bioinorganic and Synthetic Chemistry, School of Chemistry, Sun Yat-Sen University, Guangzhou 510275, P. R. China.

Section 1. Calculations

1. Calculation of the areal specific capacitance of the single electrode

(1) The areal specific capacitance of the electrodes was calculated from the CV curves using Equation (1).

$$C_s = \frac{Q}{\Delta U \times S} \qquad (1)$$

where C_a (mF/cm^2) is the areal specific capacitance, Q is the average charge during electrode charging and discharging, ΔU (V) is the working voltage window (0.8V) of the electrode, and S (cm^2) is the test area of the electrodes.

(2) The mass specific capacitance of the electrodes was calculated from the CV curves using Equation (2).

$$C_S = \frac{Q}{\Delta U \times m} \qquad (2)$$

where C_s *(F/g)* is the mass specific capacitance, Q is the average charge during electrode charging and discharging, ΔU is the voltage range (0.8V), and m is the mass of the electrode.

(3) The areal specific capacitance of the electrodes was calculated by GCD using Equation (3).

$$C_a = \frac{I \times \Delta t}{\Delta U \times S} \qquad (3)$$

where I is the current during electrode discharging (A), and Δt (s) is the discharge time of the electrode, ΔU is the voltage range (0.8V), and S (cm^2) is the test area of the electrodes.

(4) The mass specific capacitance with respect to three-electrode configuration is derived from GCD based on Equation (4).

$$C_s = \frac{I \times \Delta t}{\Delta U \times m} \qquad (4)$$

where I is the current during electrode discharging (A), and Δt (s) is the discharge time of the electrode, ΔU is the voltage range (0.8V), and m is the mass of the electrode.

(5) The healing efficiency (η, %) was calculated by Equation (5).

$$\eta = \frac{C_h}{C_0} \times 100 \qquad (5)$$

where C_0 and C_h are the specific capacitance of the original and the healed electrodes, respectively.

2. Calculation of area specific capacitance, power density, and energy density of the fully self-healable CS@PA-SC device

(1) The area specific capacitance was calculated from Equations (6).

$$C_{cell} = \frac{1}{2} \times C_a \qquad (6)$$

where C_{cell} is the area specific capacitance of the device, C_a is areal specific capacitance of the electrode.

(2) The energy density (E, Wh/cm^2) and power density (P, W/cm^2) were calculated by the equations (7) and (8).

$$E = \frac{1}{8} \times C_a \times (\Delta U)^2 \qquad (7)$$

$$P = \frac{3600 \times E}{\Delta t} \qquad (8)$$

where C_a is areal specific capacitance of the electrode, ΔU is the voltage range (0.8V).

Section 2. Curves and Figures

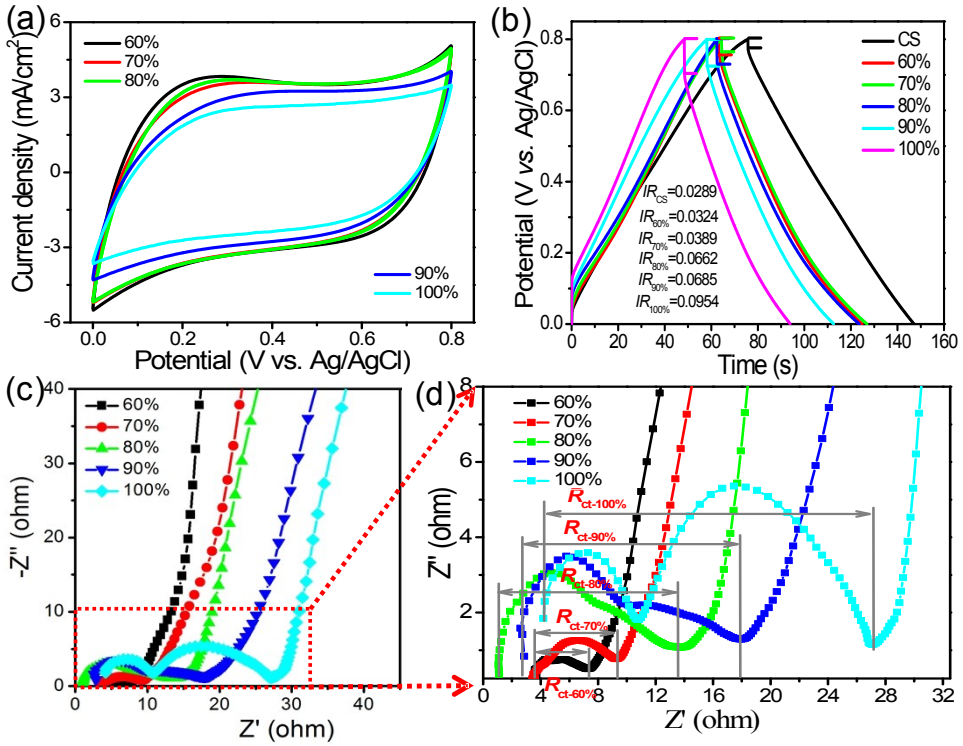

(e)

Different filling content (%)	R_{ct} value (ohm)
60%	2.322
70%	4.965
80%	11.94
90%	14.793
100%	22.869

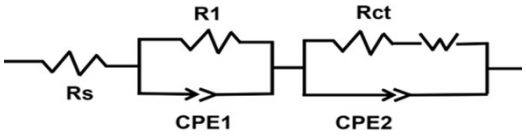

Fig. S1 (a) CV curves of CS@PANa-Fe^{3+}-LiCl electrodes with different filling weight ratio at scanning rate of 50 mV/s; (b) GCD curves of CS@PANa-Fe^{3+}-LiCl electrodes with different filling weight ratio at current densities of 2 mA/cm^2; (c, d) Nyquist plots and partly enlarge of CS@PANa-Fe^{3+}-LiCl electrodes with different filled weight ratio; (e) Fitted equivalent circuit of the CS@PANa-Fe^{3+}-LiCl electrode with different filling content of PANa-Fe^{3+} hydrogel.

Note to Fig. S1. For the CS@PANa-Fe^{3+}-LiCl electrode, its self-healing performance depends on the in-situ generated PANa-Fe^{3+} hydrogel. Therefore, in theory, if the filling amount of PANa-Fe^{3+} is larger, the self-healing performance of CS@PANa-Fe^{3+}-LiCl electrode is better. From the perspective of electrochemical performance, on the other hand, the CS@PANa-Fe^{3+}-LiCl electrode has better capacitance characteristics and smaller resistance value when the filling amount of PANa-Fe^{3+} is 60%. However, considering the two factors of self-healing and electrochemical performance of the CS@PANa-Fe^{3+}-LiCl electrode, the optimal filling amount was determined to be 70%. In addition, the R_{ct} value of the CS@PANa-Fe^{3+}-LiCl electrode also further confirmed that the conductivity of the electrode gradually deteriorated with the increase of the filling amount.

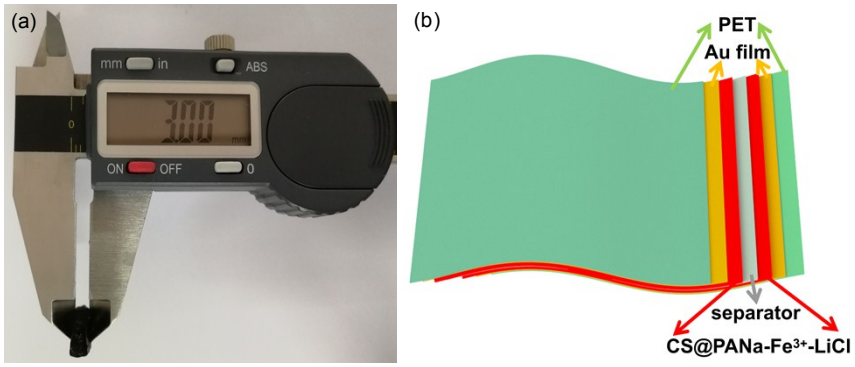

Fig. S2 (a) Optical image of measuring the thickness of CS@PANa-Fe^{3+}-LiCl electrode with Vernier caliper; (b) Schematic diagram of a fully self-healable supercapacitor fabricated by the CS@PANa-Fe^{3+}-LiCl integrated electrode.

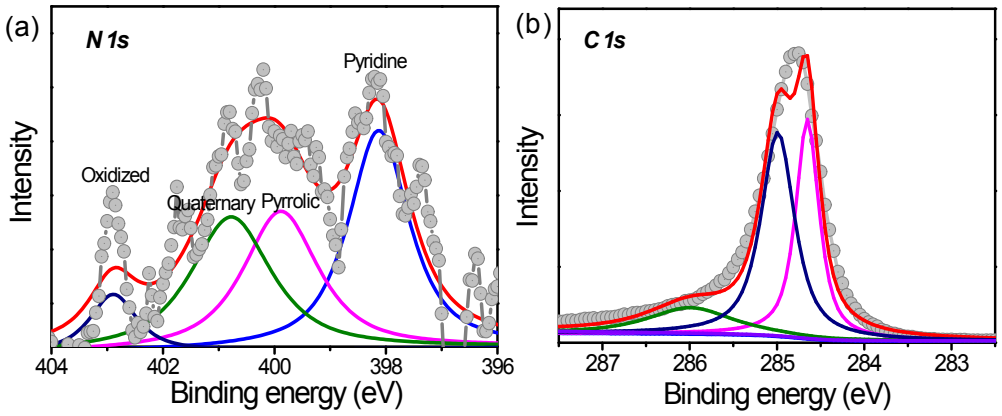

Fig. S3. High-resolution XPS spectra of CS template for (a) N 1s and (b) C 1s.

Note to Fig. S3. As shown in Fig. S3a, The N 1s spectrum can be fitted into four peaks using the Gaussian method, which indicated four components attributed to pyridinic nitrogen (N-6), pyrrolic (N-5), quaternary (N-Q), and oxidized pyridinic nitrogen (N-X).[1, 2] In the C1s spectrum (Fig. S3b), the dominant peak located at 284.6 is characteristic of the graphitic carbon (C–C), and the peak at 286.1 corresponds to C–O/C–N.[2, 3] The results indicate that the CS template is a nitrogen and carbon-rich product.

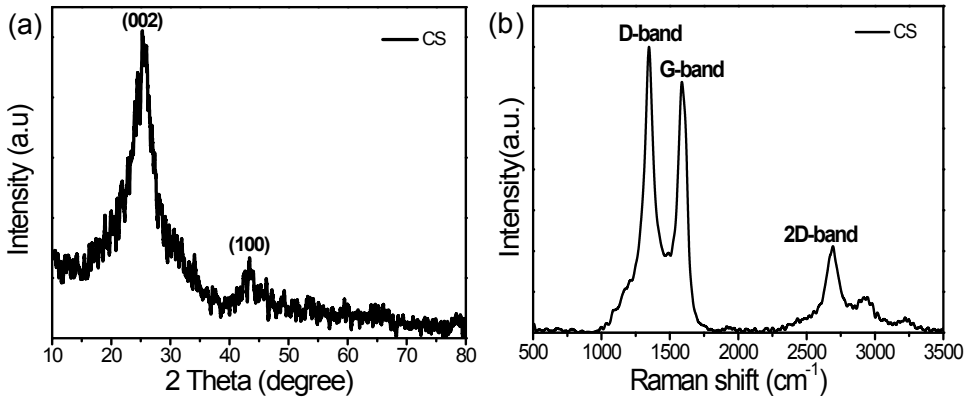

Fig. S4. XRD spectra of CS template for (a) N 1s and (b) C 1s.

Note to Fig. S4. As shown in Fig. S4a, the CS sample exhibits a typical diffraction pattern characteristic of MWCNTs. A strong peak at ~26° and a weak peak located at ~42° can be observed, which correspond to the (002) and (100) planes of the graphitic phase of MWCNTs, respectively. [4] In addition, Raman are widely used to evaluate the quality of carbon materials. As shown in Fig. S4b, the G band around 1580 cm^{-1} is a characteristic feature of graphitic layers, while the D band around 1350 cm^{-1} corresponds to disordered carbon or defective graphitic structures. [2, 4] These results indicate that CS is composed of graphitized MWCNT and MF-derived amorphous carbon materials.

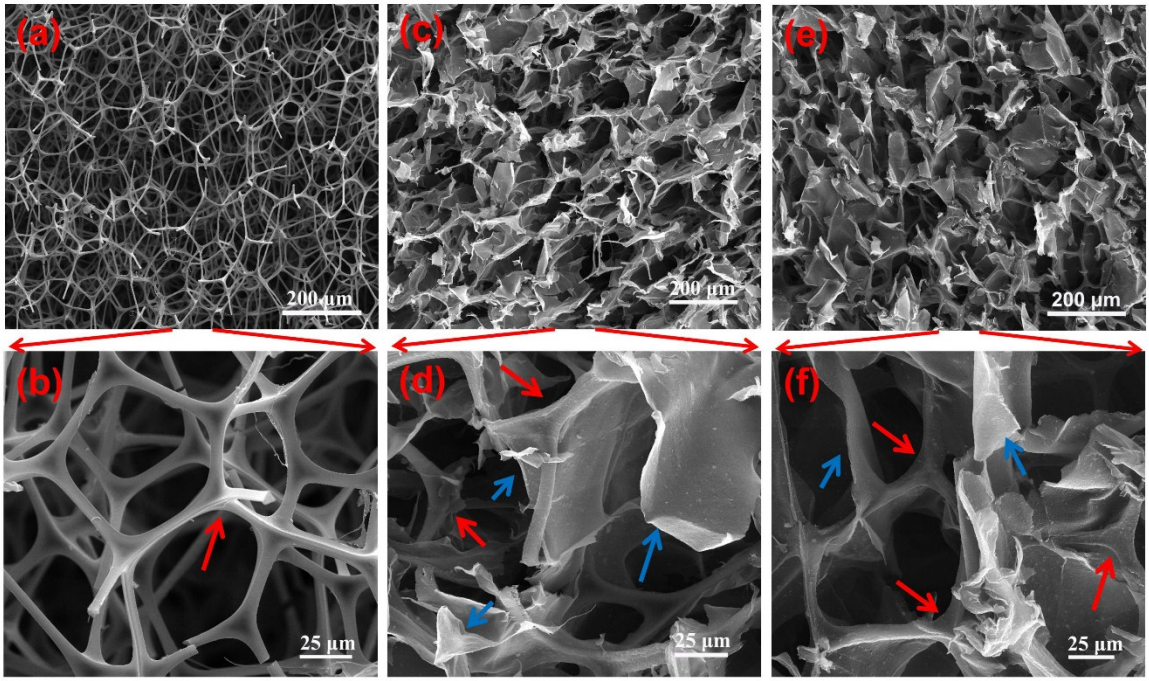

Fig. S5. SEM images with different magnification of (a, b) MF; (c, d) M-CM; and (e, f) CS template.

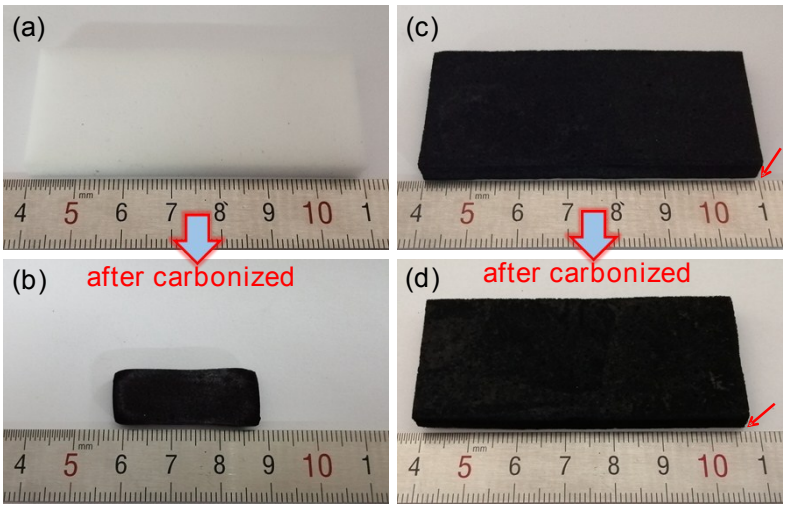

Fig. S6. Photograph of (a) MF sponge; (b) MF directly derived carbon sponge material; (c) M-CM hybrid aerogel; and (d) CS template.

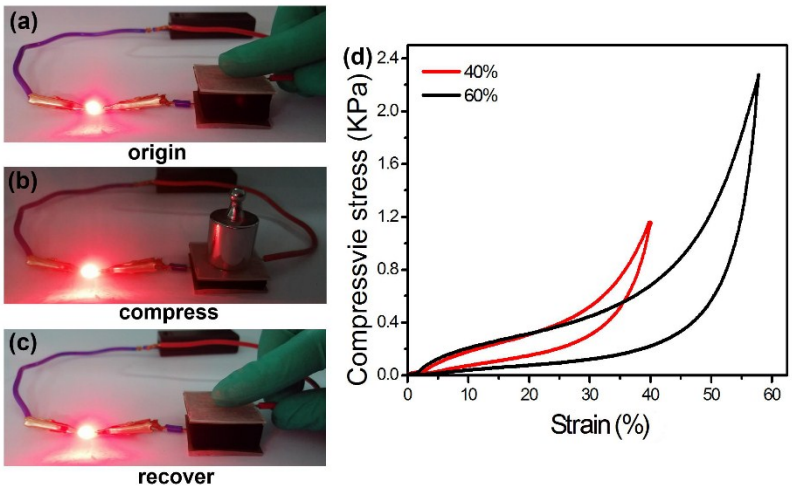

Fig. S7 (a-c) Optical images showing the CS compression and recovery process under the condition of lighted a LED; (d) Compressible stress-strain curves of the CS with different compression ratio.

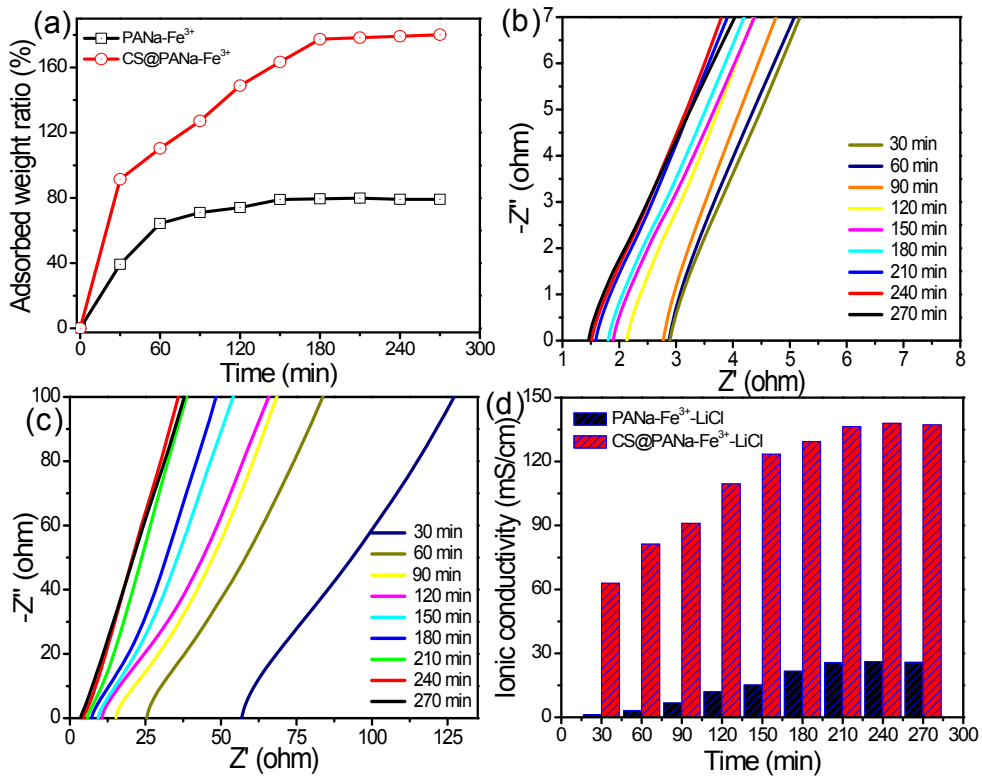

Fig. S8. (a) Comparison of adsorbed weight ratio of CS@ PANa-Fe^{3+} and PANa-Fe^{3+} after immersion in 5M LiCl solution for different time; (b) AC impedance spectrum of CS@PANa-Fe^{3+} dry gel after soaking in 5M LiCl solution for different time; (c) AC impedance spectrum of PANa-Fe^{3+} dry gel after soaking in 5M LiCl solution for different time; (d) Comparison of ionic conductivity of CS@ PANa-Fe^{3+} and PANa-Fe^{3+} after immersion in 5M LiCl solution for different times.

Note to Fig. S8. As shown in Fig. S8a, it can be clearly seen that CS@PANa-Fe^{3+} dry gel has a stronger absorption capacity of LiCl solution than PANa-Fe^{3+} dry gel, which is mainly due to CS@PANa-Fe^{3+} has a more continuous 3-D porous structures. More importantly, the conductivity of the PANa-Fe^{3+}-LiCl film is 26.0 mS/cm after soaking into LiCl solution for 240 min, while the conductivity of the CS@PANa-Fe^{3+}-LiCl electrode is high up to 137.9 mS/cm after soaking into LiCl solution for 240 min. This further shows that the integrated CS@PANa-Fe^{3+}-LiCl electrode also can fundamentally serve as a solid-state electrolyte for the storage of ions.

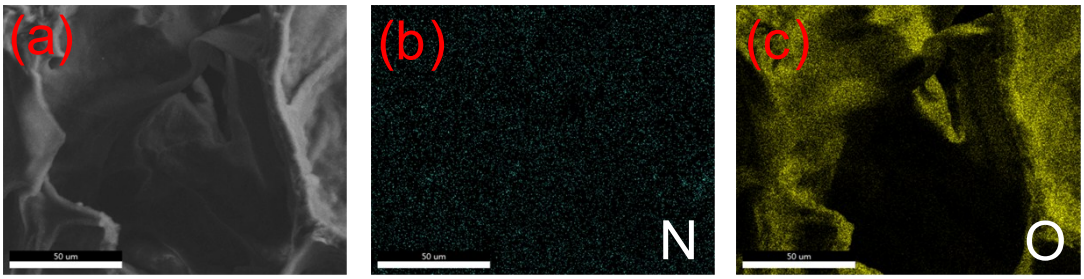

Fig. S9. SEM-EDS elemental mapping images of CS@PANa-Fe^{3+}-LiCl electrode.

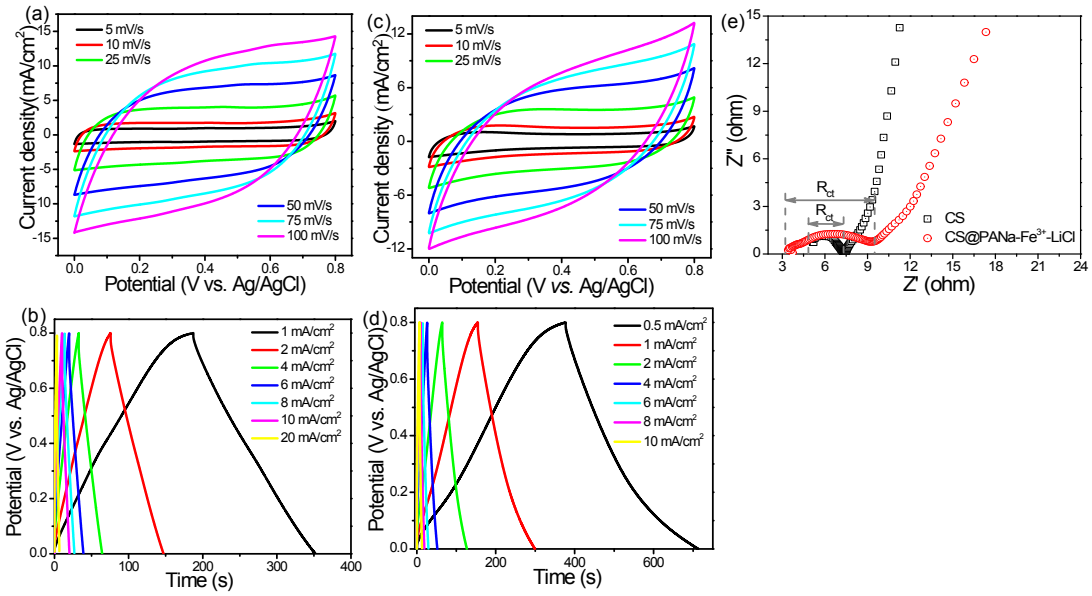

Fig. S10. (a) CV curves of CS electrode for scanning rates of 5–100 mV/s; (b) GCD curves of CS electrode at different current densities of 1–20 mA/cm^2; (c) CV curves of CS@PANa-Fe^{3+}-LiCl electrode for scanning rates of 5–100 mV/s; (d) GCD curves of CS@PANa-Fe^{3+}-LiCl electrode at different current densities of 0.5–10 mA/cm^2; (e) Nyquist plots of CS and CS@PANa-Fe^{3+}-LiCl electrode.

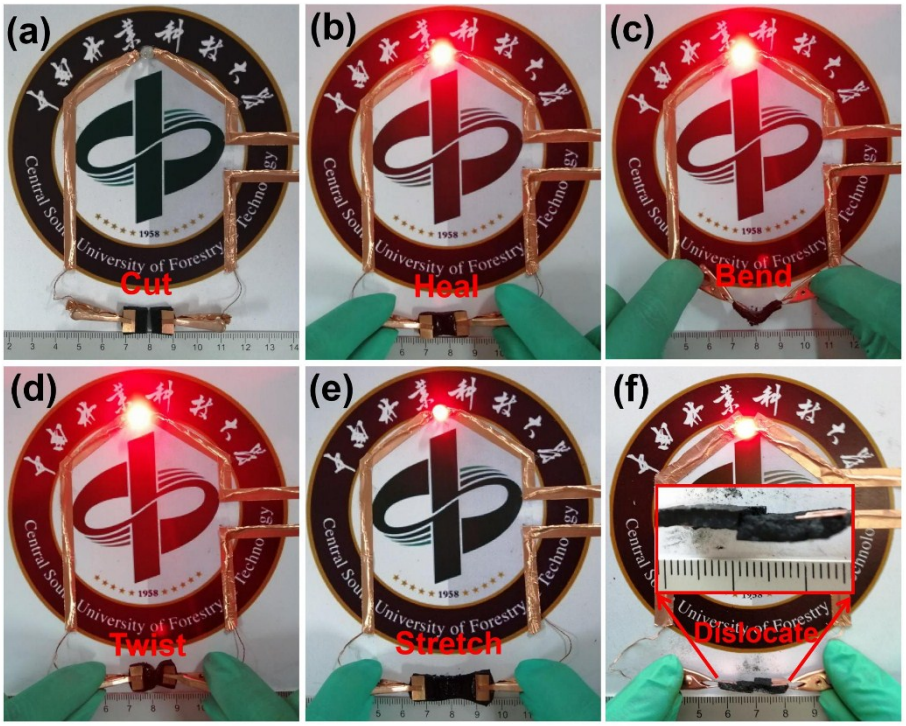

Fig. S11. Optical images of the CS@PANa-Fe^{3+}-LiCl electrode as a wire lighted a LED under different conditions of (a) cut, (b) heal, (c) bend, (d) twist, (e) stretch, and (f) dislocate.

Times	R_{ct} value
Original	4.965
1st healing	3.66
2nd healing	7.70
3rd healing	14.52
4th healing	19.89
5th healing	23.64

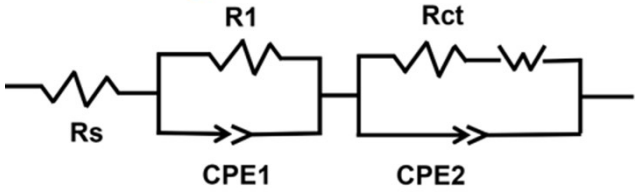

Fig. S12. Fitted equivalent circuit of the self-healing CS@PANa-Fe^{3+}-LiCl electrode and corresponding Rct value after multiple cycles of cutting and healing.

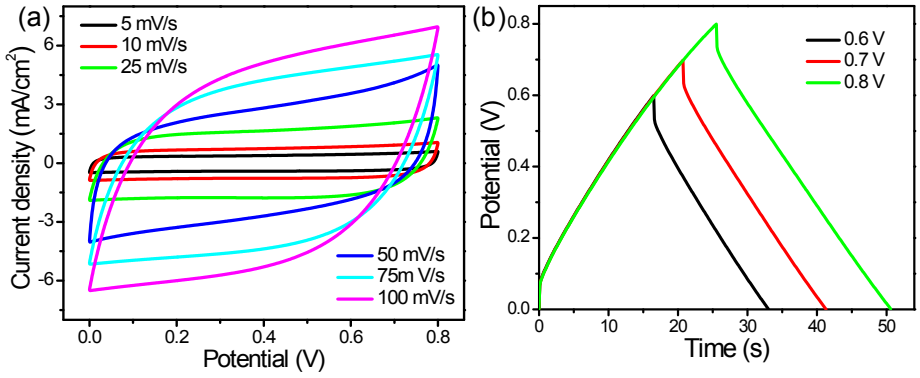

Fig. S13. (a) CV curves of CS@PA-SCs device for scanning rates of 5–100 mV/s; (b) GCD curves of CS@PA-SCs device at 2 mA cm^{-1} under different voltage windows.

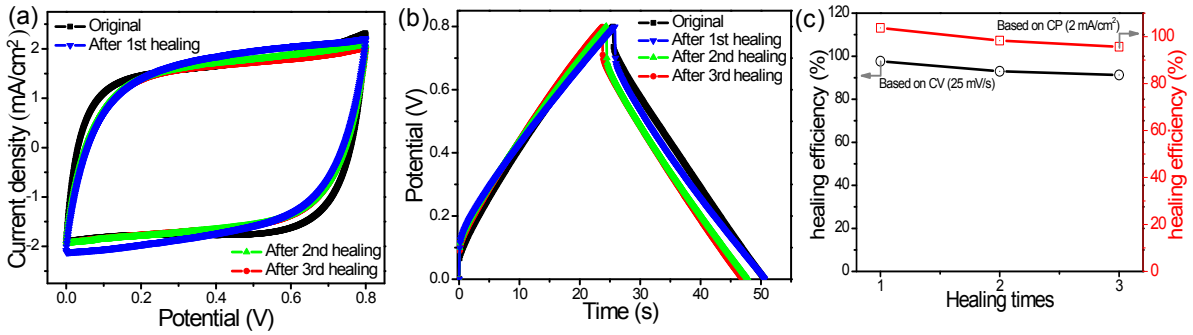

Fig. S14. CV curves of CS@PA-SCs device before and after self-healing; (b) GCD curves of CS@PA-SCs device before and after self-healing; (c) Nyquist plots of CS@PA-SCs device before and after self-healing.

Note to Fig. S14. For the purpose of proving that the fabricated CS@PA-SCs device can achieve the self-recovery of electrochemical functional characteristics, we compared the electrochemical performance of the device after three times of healing. As shown in Fig. S14a, all CV curves maintain a rectangular-alike shape of the same size, indicating that the device has good capacitance behavior after three times of healing. The comparison of GCD curves (Fig. S14b) proves that the device has good self-healing performance. In addition, the capacitance retention rates of the CS@PA-SCs device after three healing cycles are still as high as 91.3% (based on CV) and 95.7% (based on CP), respectively. These results indicate that the device has good self-healing performance (Fig. S14c).

Section 3. Table

Table S1 Wavenumber range corresponding to the characteristic functional groups.

Functional groups	Wavenumber range (cm^{-1})
-OH	3600-3200
$-CH_3$, $-CH_2$	2848, 2918
C=C	1743-1690
C-O	1650-1600
C=O	1743-1690
COO- (strong)	1580-1530
COO- (weak)	1420-1375

Note to Table S1. From the FTIR spectrum and Table S1, it can be seen that characteristic peak of –OH in the carboxyl group appears at 3440 to 3320 cm^{-1}, and two characteristic peaks of the –COO functional group are observed at 1440 and 1560 cm^{-1}, indicating formation of PANa-Fe^{3+} hydrogel. For CS template, the characteristic peaks presenting at 3417 and 1618 cm^{-1} are attributed to the stretching vibrations of O-H and C=C functional groups of the MWCNT, respectively.

Section S4. Video

Video S1 An LED indicator (3 V) lit by four units of flexible CS@PA-SCs device (size: 1 cm×1.5 cm, one CS@PA-SCs device has undergone the processing of cut and self-heal) in series.

Reference

[1] S. Chu, Y. Zhong, R. Cai, Z. Zhang, S. Wei, Z. Shao, *Small,* 2016, 12, 6724.

[2] L. Zhu, M. Gao, C. K. N. Peh, X. Wang, and G. Ho, *Adv. Energy Mater*., 2018, 8, 1702149.

[3] R. Zhang, X. Jin, Y. Chu, L. Wang, W. Kang, D. Wei, H. Li and S. Xiong, *J. Mater. Chem. A*, 2018, 6, 17730.

[4] W. Yuan, B. Wang, H. Wu, M. Xiang, Q. Wang, H. Liu, Y. Zhang, H. Liu, S. Dou, *J. Power Sources,* 2018, 379, 10.